

THE 30 MeV STAGE OF THE ARIEL E-LINAC

R.E. Laxdal, Z. Ang, T. Au, K. Fong, O. Kester, S.R. Koscielniak, A. Koveshnikov, M. Laverty,
 Y. Ma, D.W. Storey, E. Thoeng, Z. Yao, Q. Zheng, V. Zvyagintsev
 TRIUMF, 4004 Wesbrook Mall, Vancouver B.C., V6T 2A3, Canada

Abstract

A MW class cw superconducting electron linac (e-Linac) is being installed at TRIUMF as a driver for radioactive beam production as part of the ARIEL project. The e-linac final configuration is planned to consist of five 1.3GHz nine-cell cavities housed in three cryomodules with one single cavity injector cryomodule (ICM) and two double cavity accelerating cryomodules (ACM1 and ACM2) to accelerate in continuous-wave (cw) up to 10mA of electrons to 50MeV. The e-Linac is being installed in stages. A demonstrator phase (2014) consisting of a 300kV electron gun, ICM, and a partially outfitted ACM1 with just one accelerating cavity was installed for initial technical and beam tests to 22.9MeV. A Stage 2 upgrade now installed has a completed ACM1 to reach an operational goal of 3mA of electrons to 30MeV for first science from the ARIEL ISOL targets. A single 290kW klystron is used to feed the two ACM1 cavities in vector-sum closed-loop control. The paper is focused on the SRF challenges: systems design, cavity and cryomodule performance, rf ancillaries preparation and performance, LLRF and RF system performance and final beam test results.

INTRODUCTION

ARIEL[1,2] (the Advanced Rare IsotopE Laboratory) is a decade-long project with the objective to provide three simultaneous rare isotope beams (RIB) to the ISAC facility. ARIEL-I (2010-2015) was dedicated to the construction of the e-linac and a new target hall, mass separator room, and laboratory space. ARIEL-II (2016-2022) is centred around construction of a 100 kW capable electron target station, mass separators, RIB transport to ISAC. This paper is focused on the build out of the electron-driver-beam linac to 30 MeV.

The ARIEL electron linac is housed in a pre-existing shielded experimental hall adjacent to the TRIUMF 500MeV cyclotron that has been re-purposed as an accelerator vault. The e-linac presently consists of three 1.3GHz nine-cell cavities housed in three cryomodules with one single cavity injector cryomodule and one double cavity accelerating cryomodule. An rf frequency of 1.3GHz is chosen to take advantage of the considerable global design effort at this frequency both for pulsed machines (ILC) but also for cw ERL applications (KEK e-ERL, Cornell ERL and bERLinPro).

E-LINAC DESIGN

The linac architecture is determined by the choice of the final CW beam power and the available commercial cw rf couplers at the design rf frequency of 1.3GHz. The

CPI produced coupler developed with Cornell for the ERL injector cryomodule is capable of operation at ~65kW cw [3]. The cavity design assumes two CPI couplers per cavity delivering a total of 100kW of beam loaded rf power. This sets a maximum gradient per cavity at 10MV/m for the maximum beam intensity of 10mA. Final beam specifications are set at 50MeV and 10mA with five cavities installed in three cryomodules. The e-linac is being installed in a staged way with the stages shown schematically in Fig. 1.

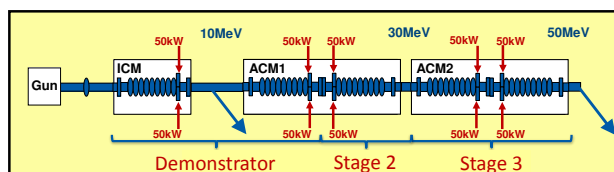


Figure 1: Schematic of the ARIEL e-Linac with staging.

The present installation is designed to accelerate in continuous-wave (cw) mode up to 10mA of electrons to 30MeV but the initial beam dumps and production targets will only be compatible with 10kW and 100kW operation respectively. First science from the targets will be produced during this stage. Stage 3, pending funding, will see the addition of a second accelerating module and a ramp up in beam intensity to the full 50MeV, 0.5MW capability.

The electron hall is shown in Fig. 2 in the present configuration. It is our intention to install a future ERL ring with injection and extraction between 5-10MeV. The angular off-set between the injector and the main linac allows accommodation of the future ring.

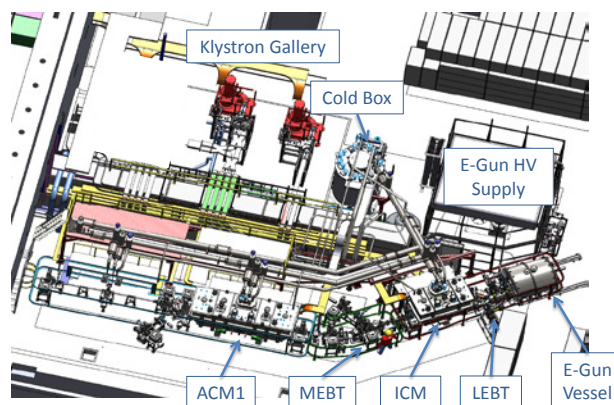


Figure 2: The present configuration of the e-Linac.

Content from this work may be used under the terms of the CC BY 3.0 licence (© 2017). Any distribution of this work must maintain attribution to the author(s), title of the work, publisher, and DOI.

Electron Gun

The electron source [4] provides electron bunches with charge up to 15.4 pC at a repetition frequency of 650 MHz. The main components of the source are a gridded dispenser cathode in a SF₆ filled vessel, and an in-air high voltage power supply. The beam is bunched by superimposing a RF modulation to overcome a DC suppression voltage on the grid.

Cavities

The cavity design parameters include $f=1.3\text{GHz}$, $L=1.038\text{m}$, $R/Q=1000$, $E_a=10\text{MV/m}$ [5]. For $Q_o=10^{10}$ the cavity power is $P_{\text{cav}}=10\text{W}$ at 2K that sets the active load requirement for the cryogenics system. A rendering of the jacketed cavity is shown in Fig. 3.

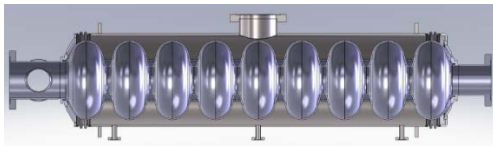


Figure 3: The e-Linac nine cell cavity with jacket.

The inner cells take their shape from the Tesla nine cell cavities but the end groups are modified to accept the two power couplers and to help push HOMs to dampers located on each end. On the power coupler end there is a stainless steel damping tube coaxial with the beam tube and extending into the beam pipe. On the opposite end of the cavity a coaxial CESIC tube is used [5]. Each tube is thermally anchored at 77K and thermally isolated from the cavity by a thin walled stainless steel bellows. The dampers are sufficient to reduce the HOMs to meet the BBU criterion (based on recirculation) of $R_d/Q \cdot Q_L < 10^7$ (Fig. 4).

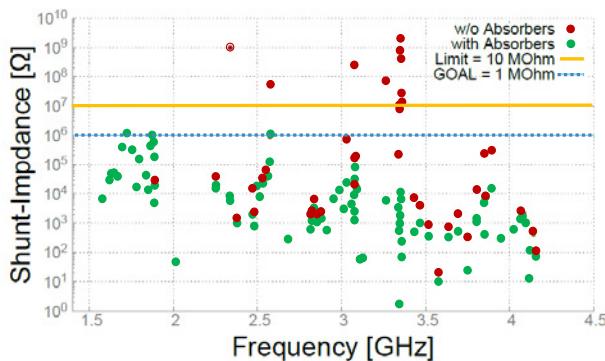


Figure 4: The simulated dipole shunt impedances without and with the absorbers compared against the BBU thresholds.

The beam tube diameters on the coupler end and opposite end are 96mm and 78mm respectively. The vacuum jacket is made from Ti with a machined two convolution flexure on either end. A single 90mm diameter chimney allows for large CW RF loads of up to 60W per cavity assuming a conservative heat transfer of 1W/cm^2 .

Cryomodule

A rendering of the EACA module is presented in Fig. 5. The cryomodule design has been reported elsewhere [6]. In brief the module is a top-loading box-like structure with a stainless steel vacuum chamber. The cold mass is suspended from the lid and includes a stainless steel strongback, a 2K phase separator pipe, cavity support posts and the cavity hermetic unit. The hermetic unit consists of the niobium cavities, the end assemblies, an inter-cavity transition (ICT) with a stainless steel HOM damper, the power couplers (FPC) and an RF pick-up. The end assemblies include the warm-cold transition (WCT), CESIC HOM damping tubes and beam-line isolation valves. Other features include a scissor jack tuner and warm motor, LN₂ cooled thermal isolation box and two layers of mu metal and alignment monitoring via a WPM diagnostic system.

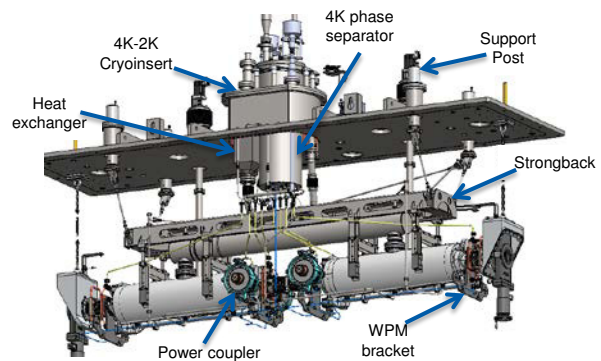


Figure 5: EACA cold mass, strong back and 4K-2K insert suspended from cryomodule top plate.

Each cryomodule is outfitted with an on-board 4K to 2K cryogenics insert. The insert consists of a 4K phase separator, a 2.5gm/sec heat exchanger and a JT expansion valve, a 4K cooldown valve and a 4K thermal intercept syphon supply and return. During cooldown the 4K valve is used to direct LHe to the bottom of the cold mass until 4K level is reached. The level in the 4K reservoir is regulated by the LHe supply valve, the level in the 2K phase separator is regulated by the JT valve and the 2K pressure is regulated by the sub-atmospheric line valve. Piping within the module delivers the syphon supply to a number of 4K thermal intercept points (WCT, ICT and FPC) and then returns the two phase LHe back to the top of the 4K phase separator.

The CPI-produced fundamental power couplers [X] developed with Cornell for the ERL Injector Cryomodule are rated for use up to 65kW cw. The design is typified by variable coupling in the range from $Q_{\text{ext}} = 0.7\text{e-}6$ to $3\text{e-}6$, two cylindrical windows, one warm and one operating near the 80K intercept, a 60 Ohm coaxial line in the cold section, and a shaped antenna tip for stronger coupling.

RF System

The RF system includes one high power rf source for each cryomodule [7]. In Stage 2 each cryomodule is driven by a dedicated 290kW CW 1.3GHz klystron CPI

VKL7967A each powered from an *Ampegon* 600kW 65kV DC supply. In Stage 3 one of these klystrons will drive ACM2 while the ICM will be driven by a 150kW power source to be determined. The basic scheme of the high power rf system for the first two cryomodules is shown in Fig. 6. A variable power divider has been employed to facilitate rf conditioning and preparation of the two 9-cell cavities in the ACM1 cryomodule prior to acceleration. Also, variable phase shifters are employed to achieve phase balance between two couplers in the same cavity and for proper cavity to cavity phasing for beam acceleration.

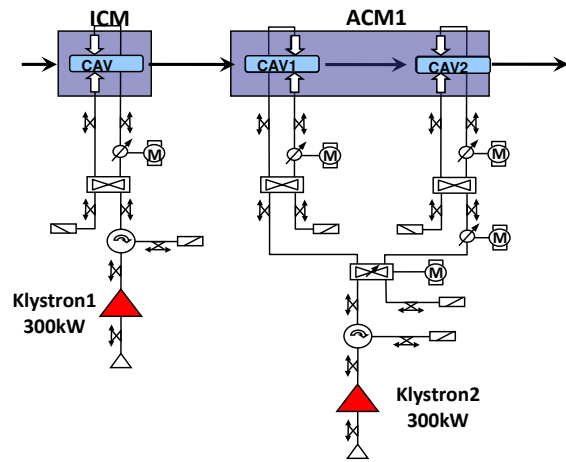


Fig. 6: The Stage-2 RF system for the ARIEL e-Linac.

STATUS

The status of the Demonstrator configuration has been reported previously [8]. In brief both the e-Gun, LEBT, ICM, MEBT, ACM1 and high energy dump were installed in 2014. At that time ACM1 was outfitted with only one SRF cavity with the second slot occupied by a 'dummy' cavity. The configuration, labelled ACMuno, was designed to provide early feedback and validation of cryogenics, HLRF, LLRF, e-Gun operation, LEBT, ICM, cryo-engineering and overall synchronization. The two cavities each reached the design specification in terms of gradient and Q_0 and acceleration was demonstrated to 23MeV at low intensities.

ACMuno → ACMduo

In 2016 the ACMuno cryomodule was removed from the e-Linac vault and moved to the cryomodule assembly area for transformation to ACMduo. The additional cavity, called ARIEL4, received a bulk BCP of 120 μ followed by an 800C, 4 hour degas, followed by a light BCP. The ARIEL4 vertical test results are shown in Fig. 7. The cavity reached a Q_0 of 8.5×10^9 at 10MV/m.

The hermetic unit of ACMuno was removed and delivered to the clean room for removal of the 'dummy' cavity and replacement with ARIEL 4 plus all rf ancillaries including two power couplers, HOM dampers, scissor tuner, rf pick-up and diagnostics. The completed hermetic unit is shown in Fig. 8. Power couplers are conditioned, two at a

time, at room temperature using a 30kW 1.3GHz IOT (Inductive Output Tube). The couplers are installed on a waveguide box and power is transmitted through the couplers to a dummy load. Preparation involves extended bake-out (five days) at 100C with N2 flowing to cover the ceramic windows. RF conditioning involves both TW (up to 18kW cw) and SW mode (9kW pulsed) with an adjustable short. The RF conditioning typically takes ~five days.

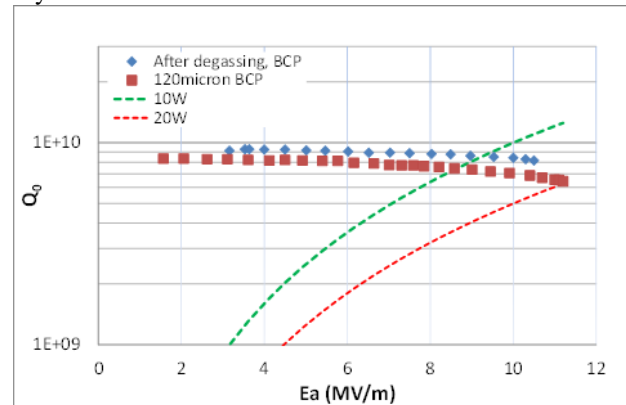


Figure 7: Vertical test result for the ACM1-2 cavity.

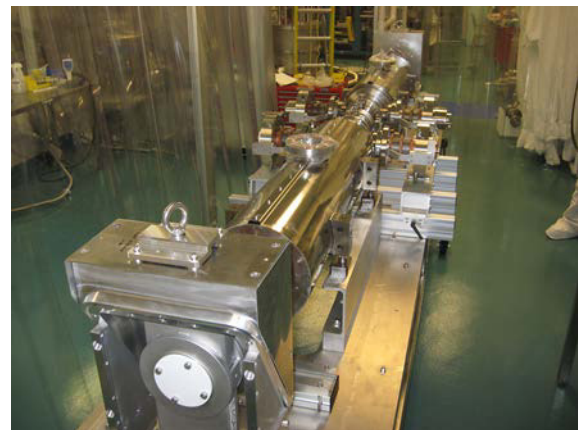


Figure 8: ACM1 cold mass assembly in the clean room.

After completion the hermetic unit is delivered to the cryomodule assembly area for mounting to the top assembly. Once the internals are completed the top assembly is lowered into the vacuum chamber. Completion of the cryomodule involves installation of the coupler warm end, bolting the end valves to the angled flanges and finishing the WPM system.

Cryogenics characterization:

Cool down to 4K and production of 2K was straightforward. The static heat loads are measured by observing the rate of falling LHe level after the supply valves are closed to the volume and noting the volume change of LHe per unit time and the heat of vaporization. The rate of 2K production is measured by closing the 4K supply valve while regulating the JT valve to keep the level constant in the 2K space. In this case the falling level in the 4K space is a combination of the static loads of the 4K and 2K space plus the vapour lost due to expansion from atmosphere to 31.5mbar.

Measured values for the ICM and the completed ACM are shown in Table 1. The 2K production efficiency improves as a function of mass flow as the temperature of the heat exchanger and JT valve decreases. The Values are 70% at 0.5g/s, 80% at 1g/s and 86% at 1.5g/s. For comparison the ACMuno cryogenics test with one cavity and one ‘dummy’ show 6.4W of static load for 4K and 6.5W of static load for 2K. The additional heat load in the ACMduo configuration is thought to come from the additional power couplers.

Table 1: Measured Cryogenics Performance for ICM and ACM

| Parameter | ICM | ACM |
|----------------|-------|-------|
| 4K static load | 6.5 W | 8.5 W |
| 2K static load | 5.5 W | 11 W |
| 2K efficiency | 86% | 86% |

Cavity characterization:

After thermalization at 2K and in situ power coupler conditioning the power divider was positioned to send all power to the new cavity. Cavity quality factors are estimated based on calorimetric measurements. The performance is presented in Fig. 9 showing RF characterization results of the new ACM1 cavity 2 (ACM1-2) compared to the previous Q measurements for the ICM and ACM1-cavity 1 (ACM1-1) cavities. The Q_0 values in the cryomodules are higher than the values measured in the vertical test. This can be due to an improved magnetic environment or different cooldown characteristic in the cryomodule configuration. The cavities meet ARIEL specifications of $Q_0=10^{10}$ corresponding to power dissipation of 10W at 2K for $E_a=10\text{MV/m}$. The results indicate that the magnetic shielding is sufficient and that the HOM dampers do not load the fundamental mode to any great degree.

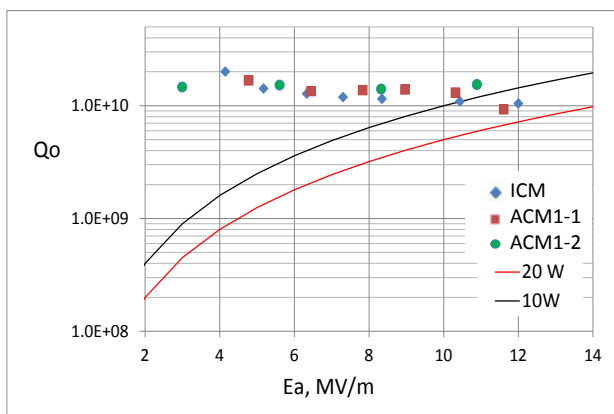


Figure 9: Results of the in situ performance tests of the three ARIEL cavities.

PREPARATION FOR ACCELERATION

The one aspect of the e-Linac operation that was not characterized in 2014 was the demonstration of driving two cavities from one klystron. In 2014 each cavity was driven from one source with one LLRF control system.

RF Set-up

Note the installed equipment indicated in the schematic of Fig. 6. A variable power divider is used to vary the power delivered to each of the two accelerating cavities for the purpose of preparing each cavity individually before powering the cavities as a tandem. The test of the power divider in terms of power delivered to the first or second cavity in ACM1 as a function of set-point is given in Fig. 10.

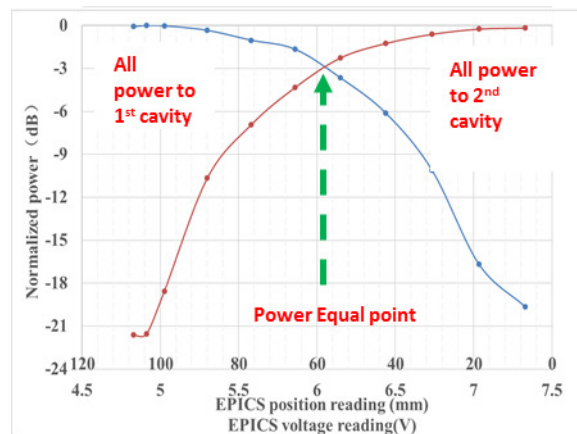


Figure 10: Test of RF power splitting between cavities.

Cavity Control

TRIUMF has a history of using the self-excited loop (SEL) [9] for LLRF. Turning on a cavity is straightforward even under extreme detuning since the SEL tracks the resonant frequency. The π -mode is selected using a band pass filter and an adjustable delay line.

Turning on the single ICM cavity is straightforward. The cavity is self-excited in π -mode and the coupler balance is optimized by varying the motorized phase shifter in one of the parallel feeds to the couplers. The optimum loop parameters are achieved ($2n\pi$ phase shift around the loop) by adjustment of the LLRF loop phase. The amplitude is adjusted to the set point and the amplitude is locked. The tuner is then used to move the resonant frequency to the set-point and the phase loop is locked. Lastly the tuner loop is locked to maintain the phase difference between the signals coupled from the forward power and the rf pick-up for zero phase shift across the cavity.

Powering up to cavities with a single SEL loop in Vector sum means the loop phases for both cavities must be kept to a multiple of 2π , irrespective of the actual phasing between the two cavities. Furthermore, the cavities could be running at different gradients based on cavity performance issues. For these reasons an additional attenuator and phase shifter are added to the second cavity feedback path to provide independent control of the loop phase and amplitude. The actual phase relationship between the two cavities for on crest acceleration can be determined individually using beam acceleration due to the relativistic nature of the beam.

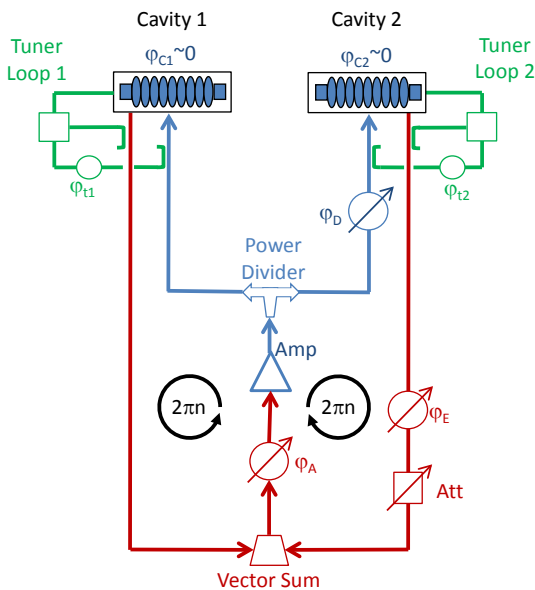


Figure 11: The LLRF loops for the two cavities of the ACM.

The two cavities each with individual tuners have to be set up separately before switching to Vector Sum (see Fig. 11). The procedure is as follows:

1. Move the power divider to send power to Cavity 1. Set up the cavity as for the ICM by balancing the coupler phases, optimizing the tuner loop phase, φ_{t1} for zero phase shift across the cavity and the loop phase φ_A for $2\pi n$ phase shift around the loop. Fix tuner 1 in this position.
2. Move the power divider to send power to Cavity 2. Set up the cavity as for ACM-Cavity1 by balancing the couplers, optimizing φ_{t2} for zero phase shift across the cavity and the loop 2 loop phase φ_E for $2\pi n$ phase shift around the loop. Adjust the loop2 LLRF attenuator to match the feedback signal strength of loop2 to loop1. Fix tuner 2 in this position.
3. Move the power divider to balance the power to each cavity and disconnect the loop 2 feedback signal. Since the power divider will introduce a phase shift φ_{B1} then loop 1 phase φ_A must be adjusted (by $-\varphi_{B1}$) for $2\pi n$ around the loop.
4. Disconnect the loop1 feedback. Since φ_A has been adjusted and the power divider introduces a phase shift φ_{B1} then loop 1 phase φ_E has to be adjusted (by $\varphi_{B1}-\varphi_{B1}$) to establish the correct SEL loop phase $2\pi n$.
5. Now both loops have the required SEL loop condition and the feedback loops can be connected. The amplitude (I) and phase (Q) of the vector sum can be locked and then the tuner loops can be optimized to the re-establish φ_{t1} and φ_{t2} and the tuner loops can be locked.

Once the Vector Sum SEL is established the exact phase relationship between cavity 1 rf and cavity 2 rf for optimal acceleration can be achieved by walking the for-

ward loop2 phase (φ_D) and countering with the loop2 feedback phase (φ_E) to maintain the SEL criterion until the correct rf phase is reached.

Status

SEL operation with the two cavities and a single source has been established and the vector sum of the two cavities in the ACM has been locked. Presently an 'auto on' script is being developed to allow automatic turn on of the two cavity summed operation. In preparation for beam operation the beam will be accelerated through the ICM and through the ACM cavities individually to get the correct phase relation between the rf and the beam for peak acceleration.

FUTURE PLANS

TRIUMF is now making plans for the next five year funding cycle starting in 2020. One such proposal is to add a recycling ring to the e-hall (Fig. 12) to allow operation in ERL mode or in RLA energy boost mode. RLA mode would be used to increase the energy for RIB production while ERL mode would be used to initiate a user program with applications such as Infra-red and Ultra-Violet Free Electron Lasers, Intense THz radiation source (FEL and/or Coherent Synchrotron Radiation (CSR)) or Compton backscattering source of X-rays.

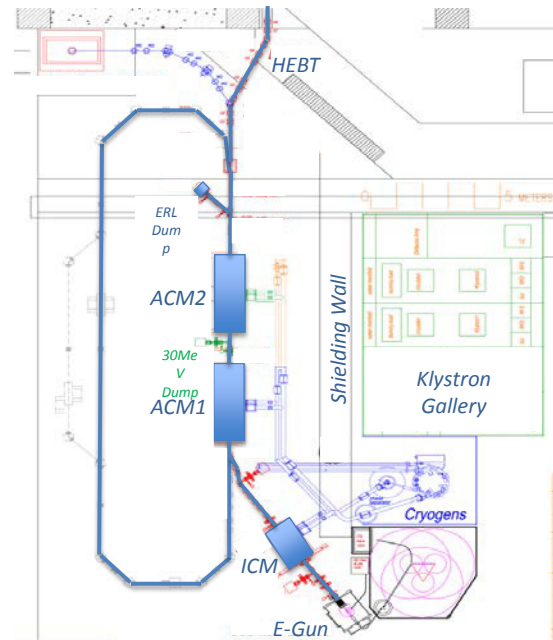


Figure 12: The e-Linac with a recirculating ring.

The ERL mode is envisaged to be done in time share with the delivery of electrons for RIB production. In this case an rf deflecting mode cavity at 650MHz would be used to selectively kick alternating 1.3GHz bunch trains in opposite directions to be separated downstream by a magnetic septum magnet for delivery to the ERL or to the ARIEL target. ARIEL bunches would be low brightness 16pC bunches at 650MHz while ERL bunches would be high brightness at up to 77pC and 130MHz and interleav-

Content from this work may be used under the terms of the CC BY 3.0 licence (© 2017). Any distribution of this work must maintain attribution to the author(s), title of the work, publisher, and DOI.

ed with respect to the ARIEL bunches (Fig. 13). A 650 MHz RF deflecting mode cavity has been designed [10] and is in final manufacture. The SRF cavity has been designed to provide up to 0.6MV transverse voltage for operation with up to a 50 MeV CW electron beam. The design was optimised for compact geometry with high shunt impedance. The separator cavity (Fig. 14) operates in a TE-like mode (H-mode), with the transverse electric field between the ridges forming the main contribution to the deflecting field. Undercuts on the ridge pull the magnetic field away from the axis reducing the negative contribution to the deflecting field from the magnetic field. This increase in shunt impedance results in increased peak electric and magnetic fields on the ridges, although these remain low for the required deflecting voltages. Another goal of the modifications was to make the cavity shorter to decrease its longitudinal footprint in the beam-line, resulting in a cavity geometry with ~50% higher shunt impedance and about half the relative length than other non-TM SRF deflecting cavity designs.

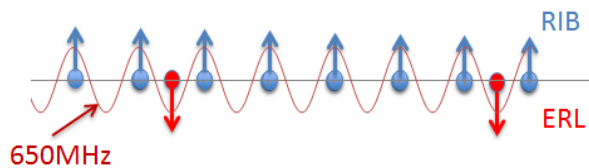


Figure 13: A possible bunch sequence for time share between ARIEL target and ERL.

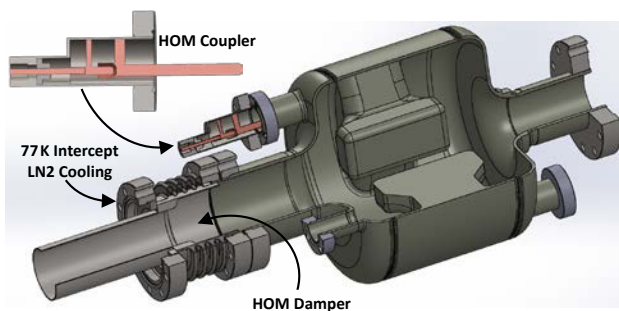


Figure 14: The H-mode RF deflecting mode cavity for ARIEL.

Due to the low dissipated power, the cavity will operate at 4 K and allows for investigations into low cost fabrication techniques.

Damping of Higher Order Modes is important due to high current CW beam. Two types of HOM dampers are used: a HOM Coupler antenna with 650 MHz filter and a HOM Damper consisting of a resistive coaxial beam pipe insert, cooled by LN2. Simulations show that the two techniques will be sufficient to damp modes to below the goal imposed by multi-pass Beam Break-Up (Fig. 15). A copper model of the cavity has confirmed the HOMs match the simulations.

The cavity is being machined from bulk reactor grade ingot Niobium and welds will be performed using TIG welding in an ultra-pure Argon chamber. RRR measurements before and after TIG welding at different Oxygen levels are used to set the requirements for welding. All

parts have been machined and should be welded in the coming weeks.

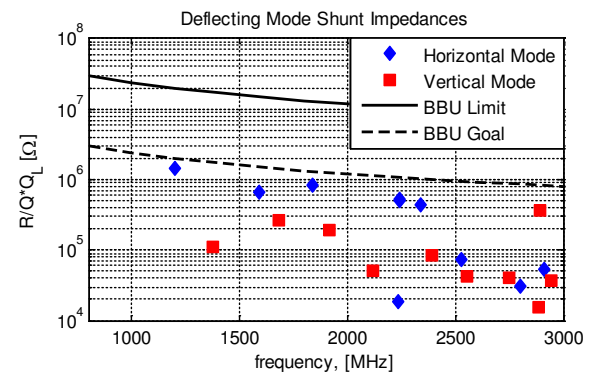


Figure 15: Calculated deflecting mode shunt impedances after employing a HOM coupler and damper (see text).

SUMMARY

The second phase of the e-Linac project is now being commissioned. The installed infrastructure will allow a final beam energy of 30-35MeV with commissioning through the summer of 2017. The plan is to ramp up the beam power to 10kW in 2018 with first beam on the radioactive production target in 2020.

TRIUMF is now in the planning phase for the next five year funding cycle starting in 2020. Projects being discussed include a second accelerating module to complete the linac to the original specification and the addition of a recirculation ring to enable ERL R&D and applications. A rf deflecting mode cavity is being fabricated to allow time share between the ARIEL beam production and the ERL beam.

ACKNOWLEDGEMENTS

We dedicate this paper to Clint Laforge a key member of our cryomodule assembly team who recently passed away due to a prolonged illness.

REFERENCES

- [1] S. Koscielniak *et al.*, “Proposal for a ½ MW electron linac for rare isotope and materials science”, in *Proc. European Particle Accelerator Conf., 2008*, Genoa, Italy, 2008, pp 985-987.
- [2] J. Dilling, R. Krucken and L. Merminga, “ISAC and ARIEL: The TRIUMF radioactive beam facilities and the scientific program”, *Hyperfine Interactions*, Vol. 225, 2014.
- [3] V. Veshcherevich *et al.*, “A high power CW input coupler for Cornell ERL injector cavities”, in *Proc. SRF’03*, Lübeck/Travemünder, Germany, Sep. 2003, paper THP38, pp. 722-725.
- [4] F. Ames *et al.*, “The TRIUMF ARIEL RF modulated thermionic electron source”, in *Proc. 28th Linear Accelerator Conf. (LINAC’16)*, East Lansing, MI, USA, Sep. 2016, paper TUPRC020, pp. 458-461.
- [5] P. Kolb, “The TRIUMF nine-cell SRF cavity for ARIEL”, PhD thesis, University of British Columbia, April 2016.

Content from this work may be used under the terms of the CC BY 3.0 licence (© 2017). Any distribution of this work must maintain attribution to the author(s), title of the work, publisher, and DOI.

- [6] N. Muller *et al.*, “TRIUMF’S injector and accelerator cryomodules”, in *Proc. SRF’15*, Whistler, BC, Canada, Sep. 2015, paper THPB115, pp. 1409-1412.
- [7] A. Mitra *et al.*, “High power RF system for e-linac for TRIUMF”, in *Proc. PAC’13*, Pasadena, USA, 2013, WEPHO01, pp. 934-936.
- [8] V. Zvyagintsev, *et al.*, “Commissioning of the SRF linac for ARIEL”, in *Proc. SRF’15*, Whistler, BC, Canada, Sep. 2015, paper TUAA02, pp. 457-461.
- [9] J. R. Delayen, “Phase and amplitude stabilization of beam-loaded superconducting resonators”, in *Proc. LINAC’92*, Ottawa, Ontario, Canada, paper TU427, pp. 371-373.
- [10] D.W. Storey *et al.*, “Fabrication studies of a 650 MHz superconducting RF deflecting mode cavity”, in *Proc. IPAC’17*, Copenhagen, Denmark, May 2017, paper MOPAB022, pp.120-122.